

HIGH-CURRENT ELLIPTICAL CAVITY DESIGN AND PROTOTYPING*

D. Meidlinger[†], J. Bierwagen, S. Bricker, C. Compton, T. Grimm, W. Hartung,
M. Johnson, J. Popielarski, L. Saxton,
National Superconducting Cyclotron Laboratory,
Michigan State University, East Lansing, Michigan, USA

Abstract

Beam instabilities due to undamped higher order modes (HOMs) in the cavities can limit the performance of high-current superconducting accelerators, including energy recovery linacs. If the accelerator is designed such that the bunch frequency is equal to the accelerating mode frequency and the beam pipe radius is chosen such that the cutoff frequency is less than twice that of the accelerating mode, all of the monopole and dipole HOMs that can be driven by the beam can be well damped. A 6-cell elliptical cavity for speed-of-light particles and a 2-cell elliptical injection cavity have been designed for such a high-current accelerator. Both cavities have an aperture 29% larger than the TeSLA cavity, at the expense of peak surface fields about 10% higher for the same gradient. The injection cavity has a geometric beta of 0.81 and was designed to accelerate electrons from 50 keV to 1 MeV, and the 6-cell cavity has a geometric beta of 1 for further acceleration. Both cavities are designed for the purpose of accelerating hundreds of milliamps without HOM-induced beam breakup and to operate at 2.45 GHz. The cavity designs and prototype injection cavity results will be presented.

INTRODUCTION

Two shapes have been designed for cavities intended for use in a high current energy-recovery linac (ERL)[1]. The first is a two-cell cavity to serve as an injector cavity, increasing the speed of electron bunches from 0.50c to c. The second is a six-cell cavity for use in the main linac. Both cavity shapes are shown in Figures 1, 2 and the figures of merit are shown in Table 1. A similar feature of both cavity designs is the large beam tube radius of 2.39 cm. This choice of beam tube radius ensures that the cutoff frequencies for the TE₁₁ and TM₀₁ modes are below the first harmonic of the accelerating mode frequency. In the scenario that every bucket of the ERL is filled, the beam would then only drive HOMs which could, with sufficient coupling, propagate out. Two copies of the 2-cell cavity, shown in Figure 3, were fabricated and tested at Michigan State University (MSU).

FABRICATION AND PREPARATION

The 2-Cell cavity was fabricated with 4 mm thick niobium (RRR=250). The flanges are NbTi using 3-3/4"

* Work supported by the NSF and the NSCL

[†] meidlind@nscl.msu.edu

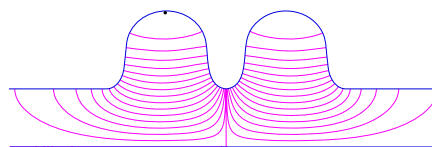


Figure 1: Electric field lines for the π -mode of the 2-Cell cavity as predicted from SUPERFISH.

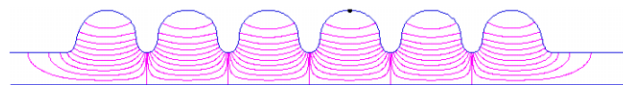


Figure 2: Electric field lines for the π -mode of the 6-Cell cavity as predicted from SUPERFISH.

ConFlat® seals. The Nb beam tubes were spun around a mandrel made of 7075 T6 aluminum. The flanges were TIG welded to the beam tubes and all remaining cavity welds were done with an electron beam. Standard copper gaskets were not used for the vertical tests, since the stainless steel flanges used for the RF input and pickup would load the cavity Q. Solid circular disks of Cu and Nb were custom made to simultaneously provide a seal between the knife edges and shield the stainless steel flanges from the cavity fields. The Nb disk was located 3.5 cm from the outer iris and contained two holes, one for the vacuum line and the other for the fixed input coupler antenna. The Cu disk was located 6.0 cm away from the other outer iris and had a single hole for the fixed pickup antenna. SUPERFISH simulations predicted a Cu disk on the pickup flange and a Nb disk on the input flange would lower the low-field Q by 20%.

Approximately 175-195 μ m of Nb was removed from the first cavity using a buffered chemical polish (BCP), followed by 70 minutes of high pressure rinsing (HPR) with ultrapure water. A small leak was detected at room tem-

Table 1: 2-Cell Cavity Figures of Merit

Cavity	6-Cell	2-Cell
E_p/E_a	2.19	2.16
B_p/E_a	4.68 $\frac{\text{mT}}{\left(\frac{\text{MV}}{\text{m}}\right)}$	4.59 $\frac{\text{mT}}{\left(\frac{\text{MV}}{\text{m}}\right)}$
$\beta_{\text{geometric}}$	1.0	0.805
R/Q	535 Ω	165 Ω
Geometry Factor	275 Ω	228 Ω
Cell-to-Cell Coupling	3.9 %	2.8 %
Frequency	2.45 GHz	2.45 GHz
Beam tube radius	2.39 cm	2.39 cm

perature which permitted the cavity vacuum during testing to be maintained above 2.2 K, but testing below the lambda point was not possible. After the initial round of testing, the first cavity was removed from the dewar and the knife edges on the two cavity flanges were polished. One of the stainless steel flanges on the vacuum line was also replaced after a small nick was discovered on the knife edge. No leak was detected at room temperature or at 90 K after polishing the cavity flanges. The cavity was reetched, removing approximately 60 μm of Nb, followed with 75 minutes of HPR. During the next vertical test, the cavity vacuum was stable down to and below the lambda point. The second cavity had approximately 190 μm removed with a BCP, followed with 75 minutes of HPR.



Figure 3: 2.45 GHz 2-cell cavity.

VERTICAL TESTING

First Cavity

Figure 4 shows the CW measurements of the intrinsic Q as a function of the accelerating gradient, E_a . It appears that some soft multipacting barriers might have been encountered. At 2 MV/m, the CW measurements were not as stable and a DC current of -50 nA was detected by a bias-tee connected to the transmitted power of the cavity with no accompanying x-rays. The DC current increased with higher cavity fields. Past 4 MV/m the cavity began self-modulating with the DC current reaching -180 nA during the transient. At 6 MV/m it was possible for the transmitted power to be stable for brief periods of time with no DC current. Since the fields were stable for brief periods, it was possible to reach higher fields by pulsing the forward power. After a few minutes of pulsed power, a new stable CW measurement at higher fields was possible. This technique was used to reach the final limiting field of 8.5 MV/m.

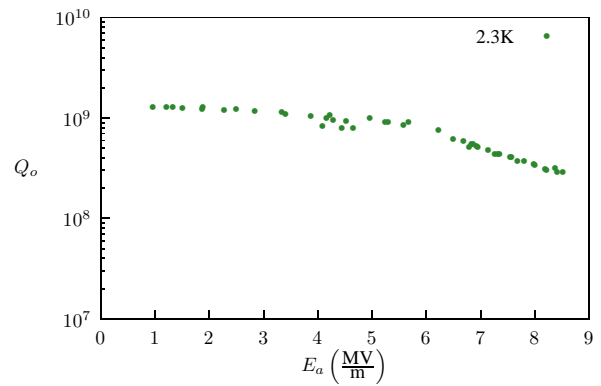


Figure 4: First round of vertical test results for the first cavity.

The next round of measurements were done after repairing the vacuum leak. Figure 5 shows the CW measurements of Q starting at 4 K, then followed by 1.83 K. The measurements became less stable at 6 MV/m, so we tried going to higher fields in the 0-mode. Returning to the π -mode, it was then possible to reach a limiting field of 7.4 MV/m. Any attempt to increase the forward power at this limit would cause the cavity to transition to a new, stable state at 1 MV/m where the Q was reduced by about a factor of 20.

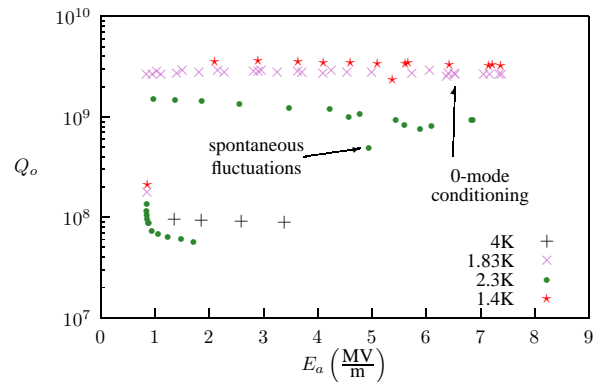


Figure 5: Second round of vertical test results for the first cavity.

The next set of measurements at 2.3 K had spontaneous fluctuations in the transmitted power occurring at 5 MV/m. At this point, the forward power was switched off and, after it was restored, the transmitted power overshoot its previous CW value by approximately 1 dB. After about 1 second the transmitted power returned to its previous, lower value but oscillating with a variation of about 0.8 dB. The transition to the low-Q state occurred at 6.9 MV/m. Increasing the forward power enabled the low-Q state to reach a limiting field of 1.7 MV/m, while reducing the forward power resulted in improving the Q at the same field level. Reducing the forward power further resulted in a sudden transition back to the high-Q state. No instabilities were observed during the measurements at 1.4 K until the low-Q state transition at 6.9 MV/m.

Second Cavity

During the vertical test at 2K, self-modulating occurred at 6.6MV/m with a small amount of x-rays (0.5-1.5 mR/hour was measured inside the radiation shield). The cavity field was reduced to 1.4 MV/m and the forward power gradually increased showing an improved Q value at 4 MV/m (see Fig. 6). This variation in Q values at 4 MV/m is also seen in Figure 4 and suggests a possible soft multipacting barrier. The transition to the low-Q state occurred at 8.7MV/m. A limiting field of 2 MV/m was reached in the low-Q state, while reducing the forward power caused the Q to improve while the field level remained constant. As the forward power is further reduced, a sudden transition back to the high-Q state also occurred.

The field at which the transition occurred was not always reproducible. The following day, an attempt was made to measure more accurately the field level at which the low-Q transition occurred. However, in this case the transition occurred at a lower limit of 8.5 MV/m. Also, after going down to 1.4K the low-Q transition occurred at 8.7 MV/m.

The zero-mode of the second cavity was also tested at 1.5K. The comparison with the π -mode is shown in Figure 7. A transition to a low-Q state occurred for both the zero-mode and π -mode, however the peak magnetic field of the zero-mode is smaller than that of the π -mode.

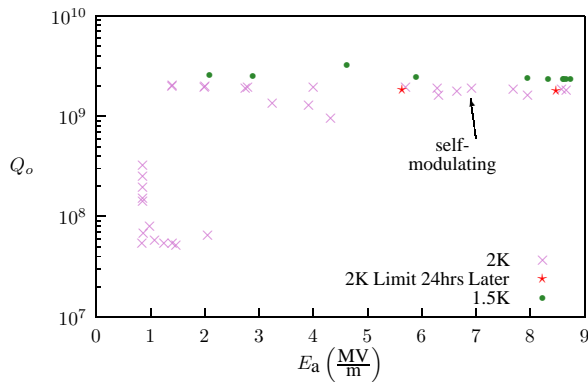


Figure 6: Vertical test results for the second cavity at 1.5 K.

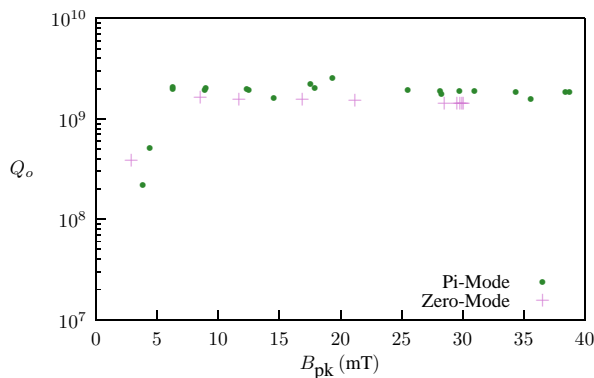


Figure 7: Low-Q transitions observed for π -mode and 0-mode of the second cavity.

DISCUSSION

The transition from a high-Q state to a low-Q state at large power levels and the transition from a low-Q state to a high-Q state at small power levels might be explained by a superconducting region of the cavity going normal-conducting at high fields. One plausible location for this to occur is the Nb disk on the input flange. The thin outer edge is the only part of the disk in direct contact with liquid He. It is possible that this contact is not sufficient for the disk to remain superconducting at high cavity fields. Prior to testing, simulations were done to predict the Q for the case that both the input and pickup flanges used Cu disks and for the case in which only the pickup flange used a Cu disk while the input flange used a Nb disk. Table 2 compares the measured ratios of Q_{low}/Q_{high} to the ratio of the Qs from the simulations. The measured Q ratios are similar to that predicted when the cavity contains two normal-conducting disks for the low-Q state and one normal-conducting disk for the high-Q state. It is also worth noting that the magnetic field at the mechanical joint of the Nb disk and the NbTi flange is 0.9 mT with a peak magnetic field in the π -mode of 40 mT. This is comparable to the 0.7 mT reached at the Nb-NbTi joint for a quarter-wave cavity tested at MSU[2] and the 1 mT reached in subsequent testing of the same quarter-wave cavity.

Table 2: Measured Q drop is comparable to that predicted from simulations for the cases of 2 Cu disks and 1 Cu disk.

Cavity	Temp. (K)	Q_{low}/Q_{high} (%)
1 st cavity π -mode	1.83	6.59
1 st cavity π -mode	2.3	9.52
1 st cavity π -mode	1.4	6.47
2 nd cavity π -mode	2.0	4.38
2 nd cavity 0-mode	1.5	6.30
Simulation	1.5	6.04

SUMMARY

Two copies of a 2-cell cavity design for high average beam currents have been fabricated and tested at MSU, achieving a maximum accelerating gradient of 8.74 MV/m. This limiting field might be explained by a superconducting region of the cavity going normal-conducting at high fields. One possible area for the superconducting to normal-conducting transition to have occurred is a Nb disk which was used to shield the stainless steel input flange during vertical testing. It seems as if some soft multipacting barriers were encountered at lower fields such as 4 MV/m, but it was possible to work through them and achieve gradients suitable for accelerating 100's of mA of beam current.

REFERENCES

[1] D. Meidlinger *et al.*, "High-Current SRF cavity design," *Physica C*, 441, 2006, p. 151-154.
 [2] W. Hartung *et al.*, "Niobium Quarter-Wave Resonator Development for the Rare Isotope Accelerator," The 11th Workshop on RF Superconductivity, Travemünde, Germany, September 8-12, 2003.